

# Design and Analysis of Low-Cost Ferrite Permanent Magnet Assisted Synchronous Reluctance Rotor and Permanent Magnet Synchronous Rotor with Flux Concentrator

S. Musuroi, C. Sorandaru, D. Vatau  
POLITEHNICA University of TIMISOARA  
Electrical Engineering Department  
Timisoara, ROMANIA

V.N. Olarescu, M. Weinman  
Diehl AKO Stiftung&Co. K.G.  
Wangen, GERMANY

**Abstract** — Rare-earth magnets which are the best solutions for PMSM rotors are expensive which makes that other types of motors are used in the applications. The solution of the replacement of these motors with PMSynRM that use low-cost type of ferrite magnets becomes more tempting lately. This paper proposes two different types of low-cost ferrite solutions: first a V permanent magnet assisted synchronous reluctance rotor (VPMSynRM) and the second a permanent magnet synchronous rotor with flux concentrator (PMSM-FC) as an alternative solution to the rare earth inserted tangential permanent magnet synchronous motor (PMSM). For the first situation, this paper proposes two topologies of PMSynRM: with one row and respective two rows of flow barriers, equipped with ferrite magnets. Finite element (FEM) approach has been utilized to show the performance of the proposed rotors. The purpose of the proposed solution is to replace only the rotor of such a PMSM that is already in production, so the size of the stator and the number of windings will remain unchanged. Finally, for the PMSM-FC, the experimental results have been shown. This one is considered competitive, taking into account the resources required for a limited-series manufacturing. The motivation of this study is to reduce the cost of the rotor by changing the type of PM and by the choice of suitable rotor geometry.

## I. INTRODUCTION

Variable speed electrical drives are currently widely used due to the rapid development of power electronics and the registered rapid growth in the field of microcontrollers ( $\mu$ Cs), digital signal processors (DSPs), and not least the digital signal controllers (DSCs). The topologies of such systems currently use especially induction machines, permanent magnet synchronous machines, synchronous machines and variable reluctance stepper motors in a variety of configurations as actuators.

The reasons for electric drive systems with variable speed for these types of motors are given by the following: the possibility of obtaining a high efficiency of drives:

- the ability to control the torque, speed or position;
- improving the transient behavior;
- the possibility to obtain application-specific drives.

The PMSM variable speed drives lead to the following advantages: obtaining a high efficiency, eliminating of an additional power supply, the possibility of obtaining high values of electromagnetic torque per volume unit, the possibility of achieving of a high performance control system [1] [2] [3] [4].

PMSM are characterized by a superior power factor and efficiency comparing to other AC machines. PMSM manufacturers choose the using a particular type of permanent magnet (PM) depending on the parameters imposed to the machine, the performances of the PM, the procurement conditions, and, particularly, the cost of the permanent magnet [1]. Now, rare earth permanent magnets and ferrites are mostly used types.

Rare earth PMs are the best technical solution for PMSM. The PM of Samarium- Cobalt has the advantage of a high residual magnetic induction, high energy density, linear demagnetization curve and a very good thermal stability. As a drawback would be the lower maximum operating temperature ( $\sim 250^{\circ}\text{C}$ ) and the higher price. PM of neodymium-iron-boron have the highest residual magnetic induction, the highest energy density and a high coercive field strength. The drawback is the low maximum working temperature ( $\sim 150^{\circ}\text{C}$ ) and the possibility of oxidation. With their help we can build PMSM with a lower weight due to high energy density [1], [5]. In conclusion, rare earth magnets substantially increase the cost of electric machine which requires the use of other constructive solutions.

Ferrite PM is an alternative to the construction of PMSM due to their low price and the fact that they are easy to be produced. Ferrites have a linear magnetization curve, a moderate maximum operating temperature ( $\sim 350^{\circ}\text{C}$ ), but the residual magnetic flux density is low. The result is a high volume and weight machine.

Variable reluctance synchronous machines (SynRM) are salient pole synchronous machines with a rotor without excitation winding, designed so that the magnetic reluctances in the two d and q-axis are different.

The producing of the SynRM electromagnetic torque is based on the shape anisotropy process, which characterizes the machines having a single excited armature, the other armature having geometry such that

the magnetic circuit reluctance to depend on its position. The rotor has different construction variants.

Generally, all these types aimed at obtaining different magnetic permeances in d and q axes, necessary to produce reluctance torque (reactive). The advantages of these machines are: the simplicity of the technological process, low-cost, low noise and robustness [1], [6] [7] [8]. The main disadvantages are related to the low value of developed electromagnetic torque, low value of power factor and low efficiency. SynRM electromagnetic characteristics can be improved by creating a rotor having both permanent magnets and variable reluctance, thus obtaining the permanent magnet assisted synchronous reluctance motor (PMSynRM). By this construction is achieved an improvement of magnetic characteristics such as power vs. internal torque angle, power factor vs. mechanical power and efficiency vs. mechanical power [9]. To achieve superior performance with this new topology, a PMSynRM optimization is required. A lot of valuable papers deal with the subject, such as, for example, [10], [11], [12], [13], [14], [15], and [16]. In [1] was proposed two low-cost ferrite V permanent magnet assisted synchronous reluctance rotors (VPMSynRM) as an alternative solution to the rare earth inserted tangential permanent magnet synchronous motor (PMSM). The conclusions of the paper revealed that the proposed rotor geometries with the flux barriers and ferrites are attractive, but the variant with two flux barriers (2V) seems to be more interesting and the shape of flux barriers can be easier optimized.

This paper proposes a new rotor topology with flux concentrators made of ferrite magnets as an alternative to PMSM made with rare earth magnets. This new version of the prototype is built, analyzed and compared with the topology (VPMSynRM) with two flow barriers 2V proposed by the authors in [1].

The paper is divided into 8 sections. Section II presents the mathematical model of the PMSynRM and the section III presents some design challenge considerations and the sections IV-VI synthesizes the presentation two rows flux barriers variant, extensively developed in [1] and used as a reference for comparison with the new version of rotor proposed in this paper. Section VI presents a new proposed variant of the rotor with ferrite magnets and flux concentration. Section VII shows the experimental results of permanent magnet synchronous machine with flux concentration (PMSM-FC). The last section summarizes the conclusions of the paper.

## II. THE MATHEMATICAL MODEL OF PMSYNRM

Neglecting the saturation and the core losses, the stator-voltage and flux-linkage of the PMSynRM in the dq reference frame are expressed as follows:

$$\begin{aligned} u_d &= R_s \cdot i_d + \frac{d\lambda_d}{dt} - \omega_r \cdot \lambda_q, \\ u_q &= R_s \cdot i_q + \frac{d\lambda_q}{dt} + \omega_r \cdot \lambda_d, \\ \lambda_d &= L_1 \cdot i_d + L_{md} \cdot i_d = L_d \cdot i_d, \\ \lambda_q &= L_1 \cdot i_q + L_{mq} \cdot i_q - \lambda_m = L_q \cdot i_q - \lambda_m \end{aligned} \quad (1)$$

$L_d$  and  $L_q$  are the d and q axes total inductances and  $L_1$  is the stator leakage inductance.

$\lambda_m$  is the amplitude of the linkage flux due to the permanent magnets  $\lambda_{pm}$ .

Under these conditions, the motor torque  $T$  appears as a sum of two components: reluctance (reactive) that is due to the shape anisotropy characterizing  $T_r$  and the machine excitation component due to PM,  $T_m$ :

$$T = T_r + T_m = \frac{3}{2} p \left[ (\lambda_d \cdot i_q - \lambda_q \cdot i_d) + (\lambda_{dm} \cdot i_q - \lambda_{qm} \cdot i_d) \right] \quad (2)$$

In relation (2),  $\lambda_{dm}$  and  $\lambda_{qm}$  are the d and q-component of PM flux.

## III. DESIGN CHALLENGE

The main purpose of this paper is to study the performance of the new motor obtained by combining the stator of an NdFeB inserted tangential permanent magnet synchronous motor with the proposed rotor geometries. The proposed rotor structures must be design in such a way that is possible to achieve the same torque per current ratio in the constant torque area and the same torque capability in field weakening are like with the initial PMSM with NdFeB.

The main challenge of the rotor design using ferrites is the small space available for the PM and flux barriers, because for the rotor designed with NdFeB a small PM volume is needed, so a compact PMSM can be designed.

The design is based on an existing 12 slot stator with concentrated windings and 50 mm inner diameter.

The stator length is 37 mm. The winding scheme is presented in 0.

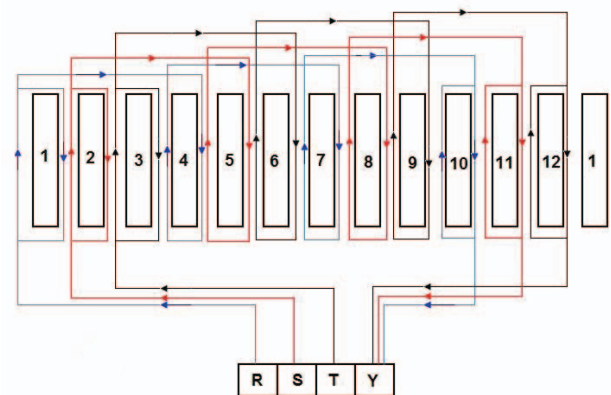


Fig.1. The machine stator winding scheme

The new rotor has the same number of poles and the same outer diameter 49.3 mm like the initial rotor.

The permanent magnet used for the new proposed rotors is a strontium ferrite FS-4 with following magnetic properties:  $B_{min} = 0.4$  T  $H_C \geq 223$  kA / m and  $(BH)_{max} = 27.2$  kJ/m<sup>3</sup>.

### A. Design strategy - PM volume

The required permanent magnet volume was calculated with the following relation [17]:

$$V_{PM} = \frac{2}{\pi^2} \cdot \frac{k_\phi \cdot k_{ad} (1 + \epsilon)}{f_s \cdot k_{um} \cdot k_{im} \cdot B_r \cdot H_c \cdot \eta_m \cdot \cos \varphi_m} \cdot k_m \cdot T_{mN} \cdot \Omega_N \quad (3)$$

where:  $k_\phi$  is the form coefficient of the permanent magnet field,  $k_{ad,q}$  is the coefficient of the magnetic reaction in the air gap,  $\varepsilon$  is the degree of excitation of the motor,  $f_s$  is the stator frequency,  $k_{um}$  is the coefficient of use of permanent magnets,  $\eta_m$  and  $\cos\phi_m$  are the efficiency and factor power the motor,  $T_{mN}$  is the rated torque,  $\Omega_N$  is mechanical speed and  $k_m$  is the motor overload factor and it can be calculated with the following relation:

$$k_m = \sqrt{1 + \frac{1}{\varepsilon^2} \cdot \left( \frac{k_{ad}}{k_{aq}} \right)^2} \quad (4)$$

#### B. Design Strategy – FEM, $L_d$ , $L_q$

The design of proposed rotors is carried out using the two-dimensional finite element software Vector Fields OPERA, so it can be considered the nonlinear magnetic behaviors of the materials which play a key role in the motor performance prediction.

By the movement of the rotor over the stator slot pitch, the back EMF, cogging torque and the torque ripples caused by permeance variations are taken into account.

A standstill method is proposed to simulate the direct d- and quadrature q-axis inductances with the FEM software. For a nonlinear magnetic material, the inductance is depending on the level of a current.

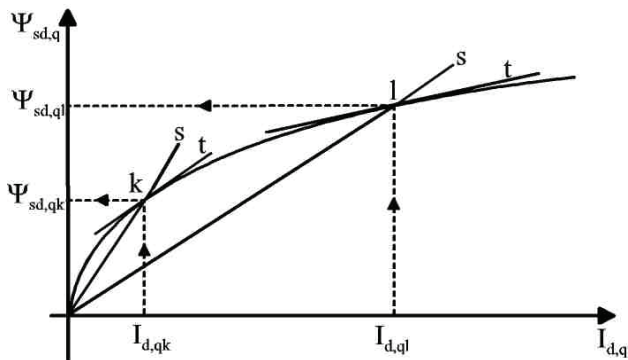


Fig. 2. Nonlinearity of d- and q-axis inductances

Fig. 2 shows the variation of the d- and q-axis magnetic flux versus d- and q-axis current. The inductance in the point “k” can be calculated using the following relation (“tangent” inductance):

$$L_{d,qkt}(I_{d,qk}) = \frac{d\Psi_{sd,qk}}{dI_{d,qk}} \quad (5)$$

The d- and q-axis stator flux linkage can be calculated with the following relation:

$$\Psi_{sd,qk} = \int_0^k (U_{sd,q} - R * i_{d,q}(t)) dt \quad (6)$$

#### IV. VPMSYNRM WITH ONE V FLUX BARRIERS

Variant analysis assumes a total volume of magnet calculated  $V_{PM} = 39587.37 \text{ mm}^3$ .

Magnet fills the entire barrier (green area in Fig. 3).

FEM modeling and simulation were done using Vector Fields OPERA platform.

FEM model of 1V version is shown in Fig. 3.

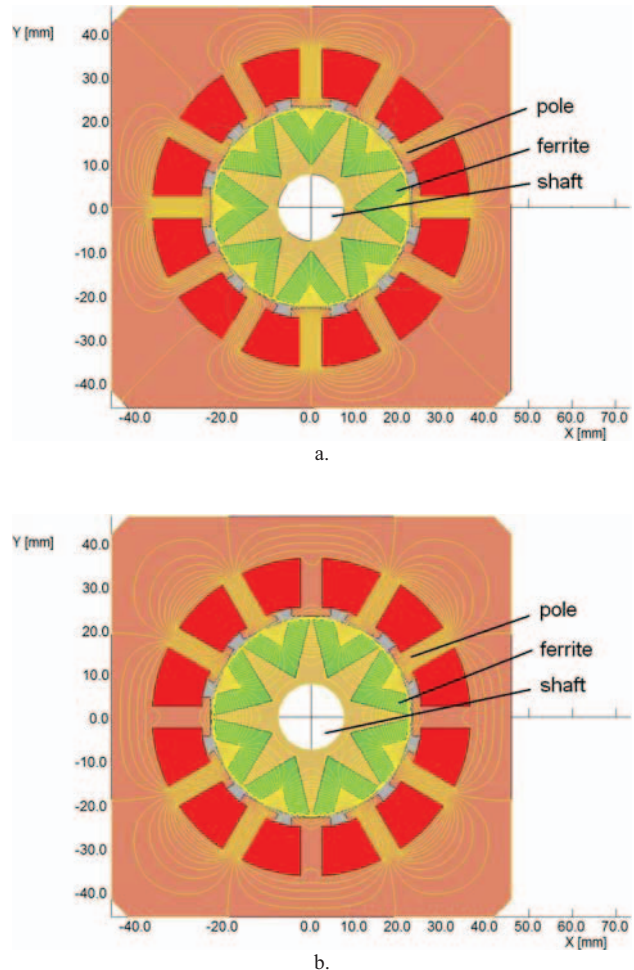


Fig. 3. 1V model variant with increased magnet volume - a. d-axis, b. after q axis.

It can be observed the path field lines for the situation in which the rotor is placed in d axis or q axis. For the two positions of the rotor, the distribution of the induction in the air gap has been simulated and the results are presented in Fig. 4.

The analysis of the Fig. 4 it results that this rotor structure allows the obtaining an induction of 0.4 T peak in the machine air gap. The following is obtained for the back-EMF simulations (see Fig. 5.a) and cogging torque (see Fig. 5.b).



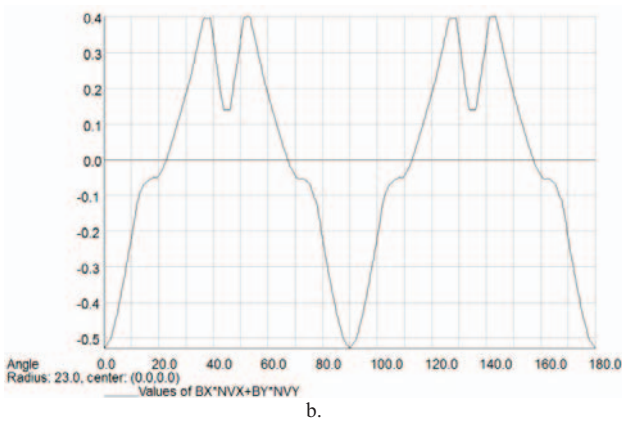
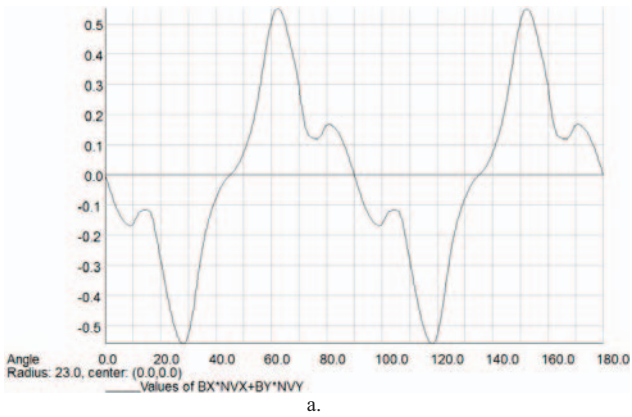


Fig. 4. Flux distribution: a. d-axis, b. q-axis

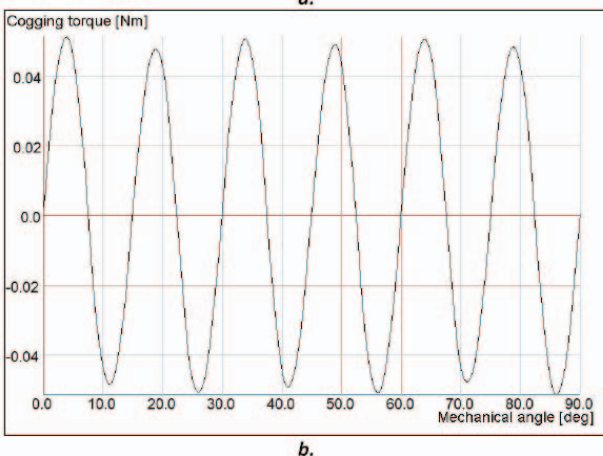
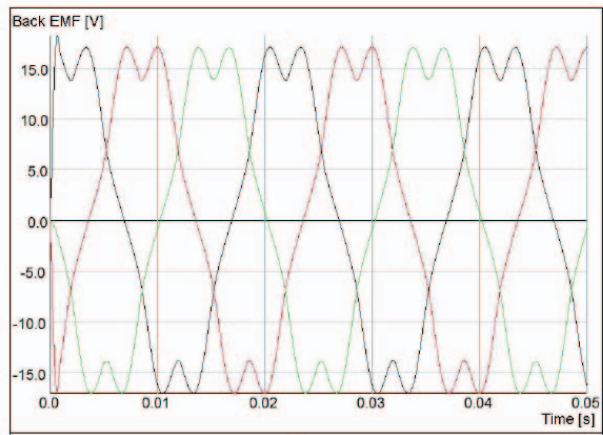


Fig. 5. a. Back-EMF, b. Cogging torque.

Simulations show good values for both the back EMF and cogging torque. Fig. 6 shows the curves inductance  $L_d$  (a) and  $L_q$  (b) versus currents  $I_d$  and  $I_q$  respectively and Fig. 7 presents the variation of phase inductance for current  $I = 4$  A, depending on the rotor position expressed in electrical angle.

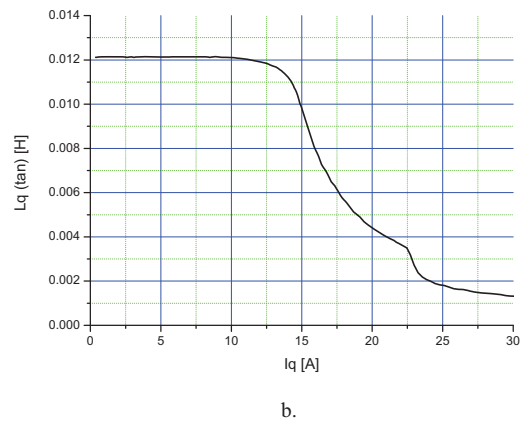
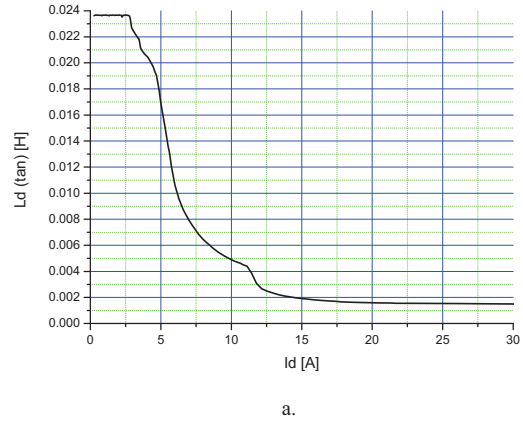


Fig. 6. a.  $L_d$  and b.  $L_q$  inductivities curves vs. currents

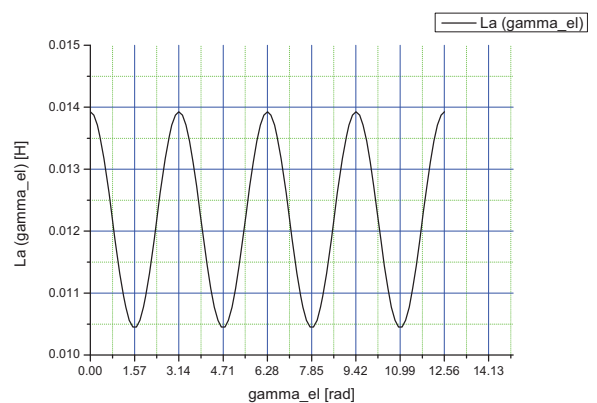
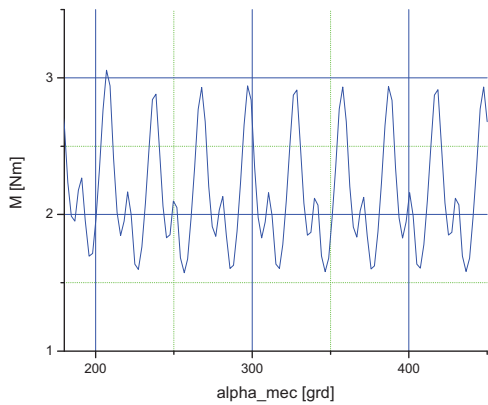
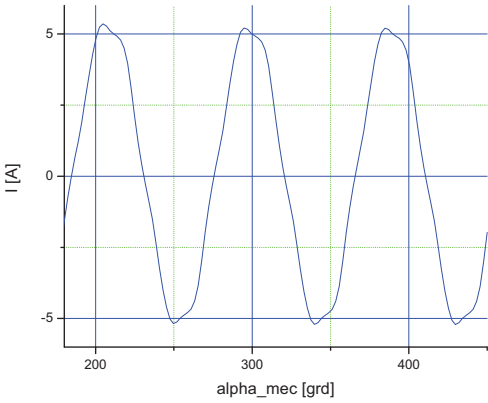


Fig. 7.  $L_a = f(\gamma_{el})$  at  $I = 4$  A.

For inductance following values were obtained, for a current of 4 [A]:  $L_d(\tan) = 20.49$  [mH],  $L_q(\tan) = 11.96$  [mH] a ratio  $L_d / L_q = 1.71$ . For determining the inductance, the tangent method as been used. Fig. 8 a and b presents the variation of torque and current for different loads, simulated by different angle loads. Simulations are for speed of 750 rev / min.



a.



b.

Fig. 8. a. Torque and b. Current variations with load.

Analyzing the results we can say that 1V model can be regarded as a viable alternative for a cheap PMSynRM type using ferrite magnets.

V. VPMSYNRM WITH TWO V FLUX BARRIERS - 2V

The proposed VPMSynRM-2V rotor geometry two flux barriers in paper [1] are filled with ferrite. The stator remains unchanged as topology and geometric dimensions and the characteristics of material used are the same with the initial PMSM with NdFeB.

In this case of the proposed rotor with two flux barriers are proposed actually two different variants (see Fig. 9a and b):

- the first variant (2V) has two flux barriers with the same width (2 mm), and the volume of the permanent magnet is  $V_{PM} = 29325.04 \text{ mm}^3$ ;
- the second variant (2VU) has also two flux barriers but the width of these two flux barriers is different (2.2 mm and 1.27mm), and the volume of the permanent magnet is  $V_{PM} = 24339.78 \text{ mm}^3$  (17% less volume than in the first variant).

The permanent magnet volume was determined by relations (3) and (4).

In this case the simulated distribution of the PM magnetic flux density (d-axis and q-axis) in air gap is

shown in Fig. 10 a and b for variant (2V) and Fig. 11 a and b for variant (2VU).

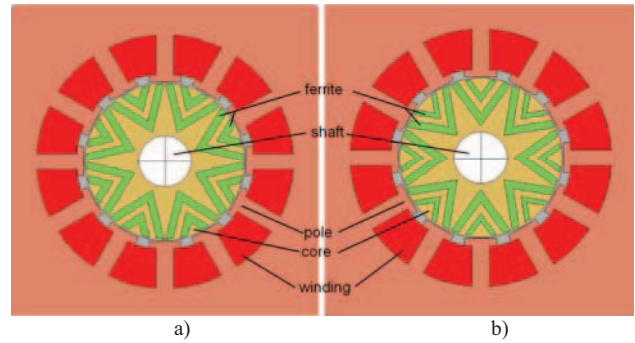
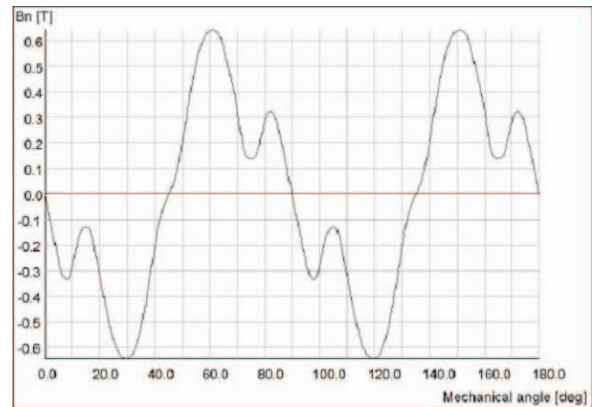
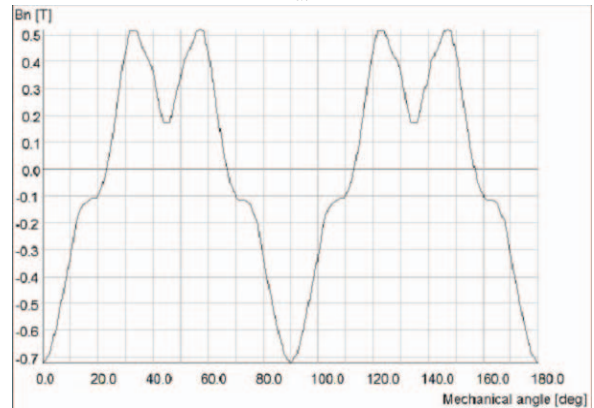


Fig. 9. Two V flux barriers rotor geometry: a. with same width of flux barriers 2V; b. with different widths of the flux barriers 2VU.

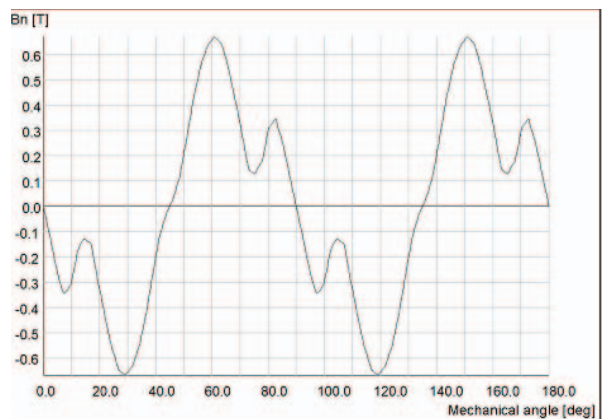


a.



b.

Fig. 10. Flux density distribution: a d-axis, b q-axis (2V).



a.

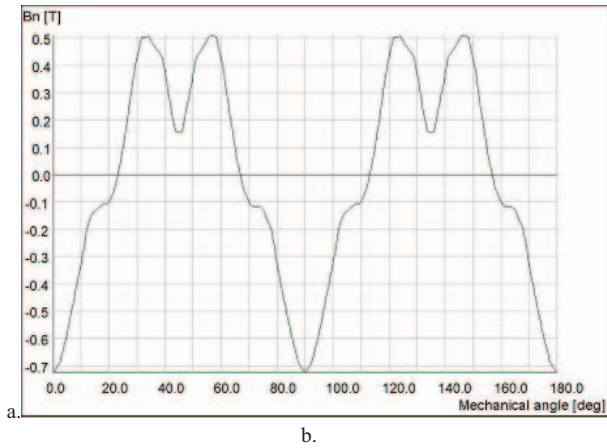


Fig. 11. Flux density distribution: a d-axis, b q-axis (2VU).

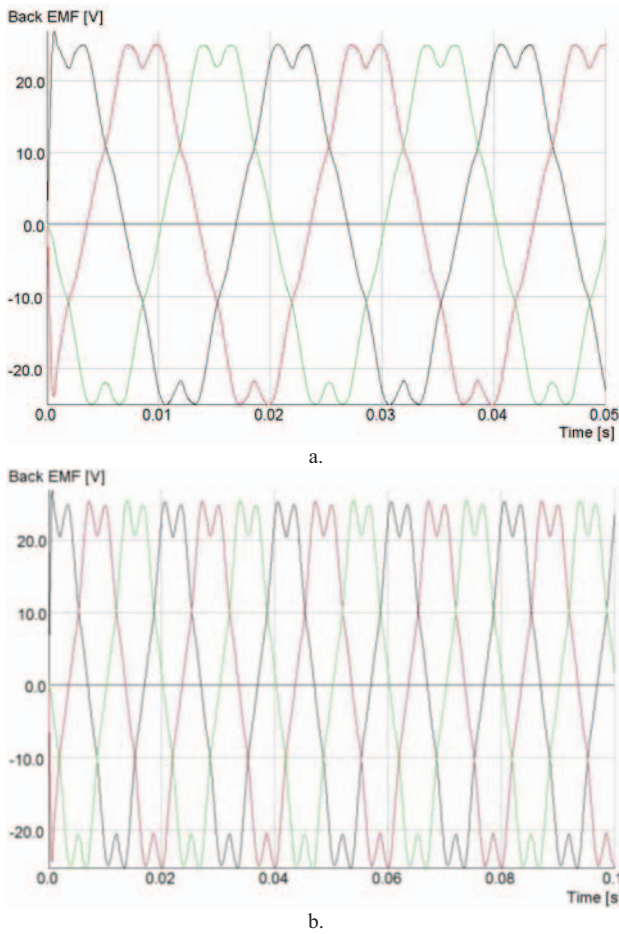


Fig. 12. Back-EMF a. 2V; b. 2VU.

Further, the curves obtained by simulation for back-EMF and cogging torque, shown in Fig. 12 and Fig. 13, will be analyzed.

The variant with two equal width barriers 2V is characterized by a peak of  $E_{pk2v}=24$  V back-EMF so an increase of 33% from 1V variant and the variant 2VU has the peak value of the back-EMF  $E_{pk2vu}=22$  V.

The permanent magnet flux linkage has the following values  $\Psi_{PM2v}=0.076$  Wb, respectively  $\Psi_{PM2vu}=0.070$  Wb

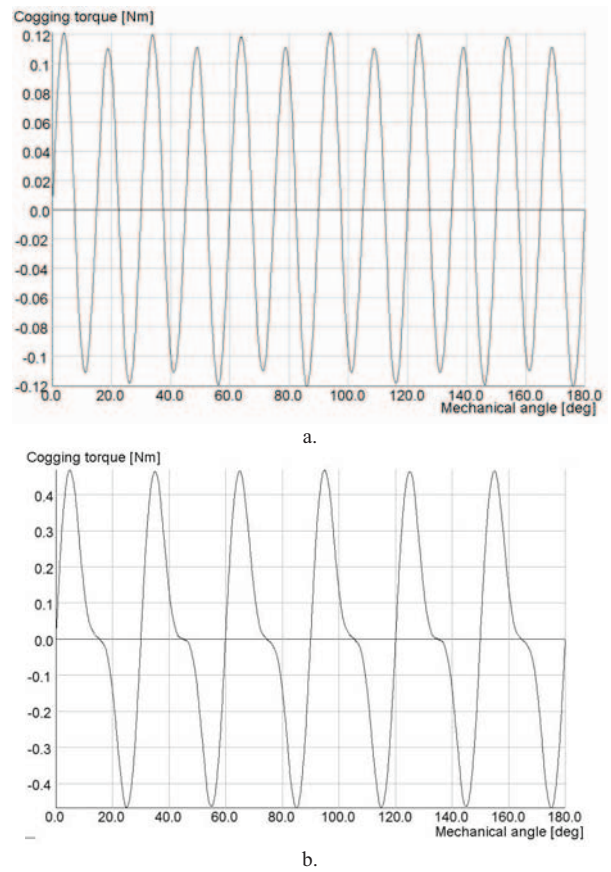
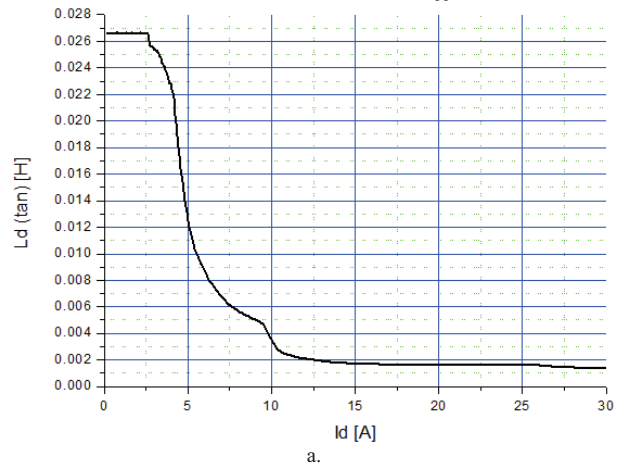


Fig. 13. Cogging torque 2V; b. 2VU

The peak value of the cogging torque for the two proposed variants with two flux barriers are  $T_{cog2v}=0.012$  Nm respectively  $T_{cog2vu}=0.045$  Nm

Fig. 14 presents the curves of inductance  $L_d$  and  $L_q$  versus currents  $I_d$  and  $I_q$  for the variant with 2 flux barriers 2V. The curves of inductance  $L_d$  and  $L_q$  versus currents  $I_d$  and  $I_q$  for the variant 2VU is not presented in this paper but the variation is near the same. For d- and q-axis inductance following values were obtained:  $L_d(4A) = 23.75$  mH,  $L_q(4A) = 15.8$  mH and the saliency ratio  $L_d/L_q = 1.50$ .

Fig. 15 presents the variation of torque caused by the permeance variations at 3.6 A in the constant torque area for the rotor variant 2V. In this case for the proposed VPMSynRM-2V rotor at 3.45 A the average torque is  $T_{av2v}=1.9$  Nm and the torque ripple is  $T_{ripple2v}=26.3\%$ .





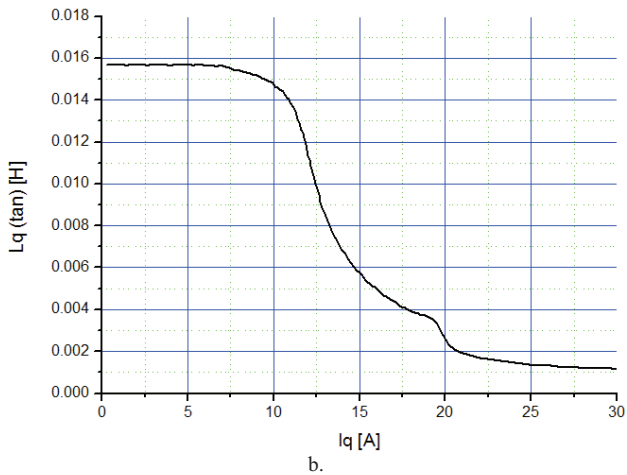


Fig. 14. The a.  $L_d$  and b.  $L_q$  inductivities curves vs. current for varian 2V.

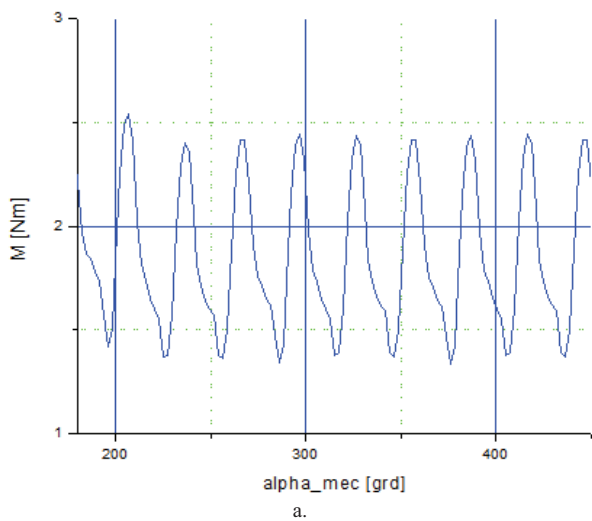


Fig. 15. Torque variation at 3.45 A.

### VI. PMSM WITH FLUX CONCENTRATOR ROTOR (PMSM-FC)

The new variant introduced by this paper is with flux concentration. This variant, which uses also ferrite PM, wants to be an alternate solution to the PMSM realized with rare earth PMs. So, in this case also, the stator remains unchanged in terms of dimensions and material characteristics. The proposed geometry is presented in Fig. 16.

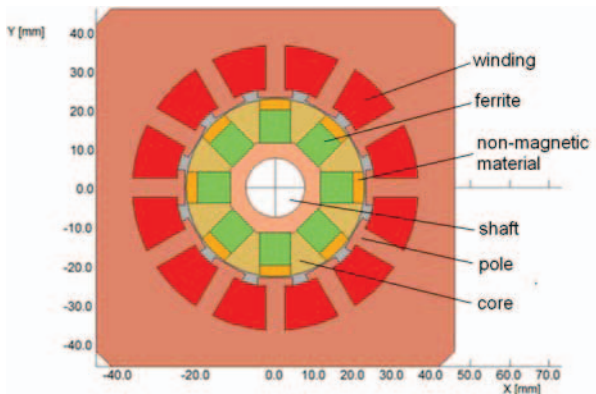


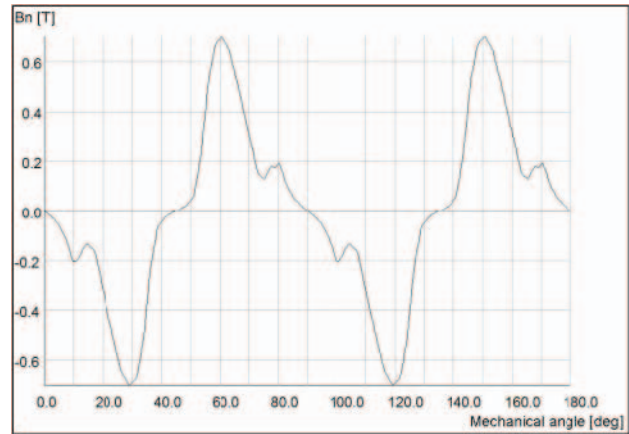
Fig. 16. PMSM wit flux concentrator (PMSM-FC)

The volume of the permanent magnet  $V_{PM} = 26481.72\text{mm}^3$  has been calculated using relations (3) and (4). It can observe a volume reduction of 9.7% comparing to the variant VPMSynRM-2V and an increase of 8% comparing to the variant VPMSynRM-2VU.

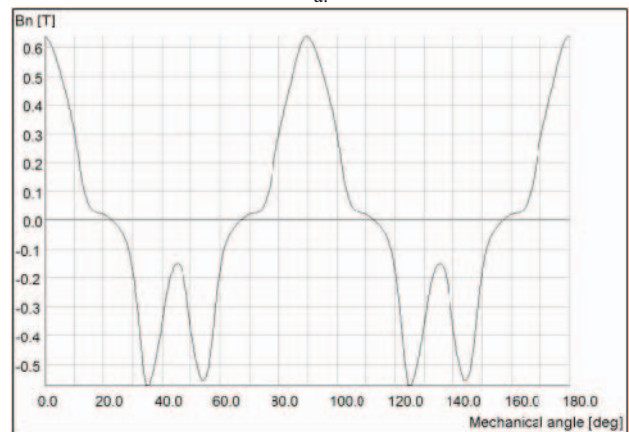
The simulated distribution of the PM flux density in air gap is shown in Fig. 17.

The peak values of the simulated d- and q-axis magnetic flux density in the air gap are greater than 0.6 T.

Fig. 18 shows the shape of the back-EMF and the shape of the cogging torque at 750 rpm.

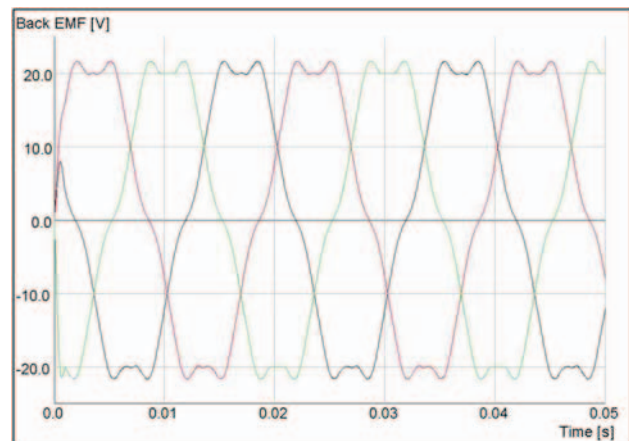


a.



b.

Fig. 17. Flux density distribution: a d-axis, b q-axis.



a.

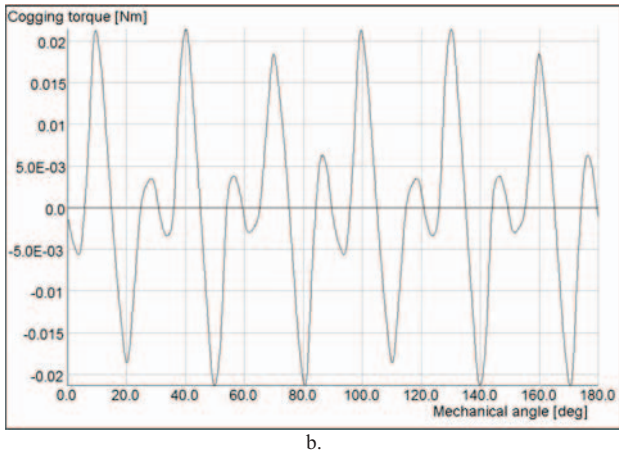
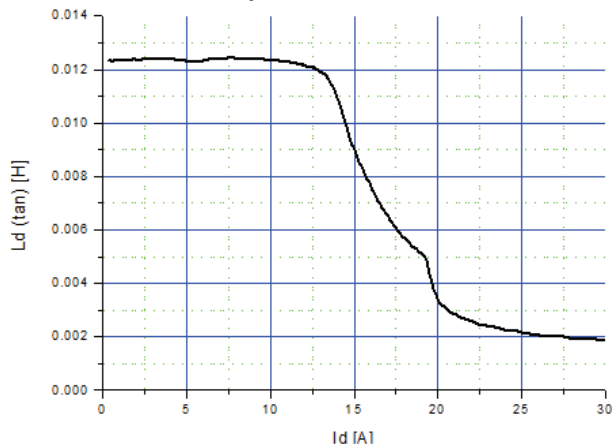


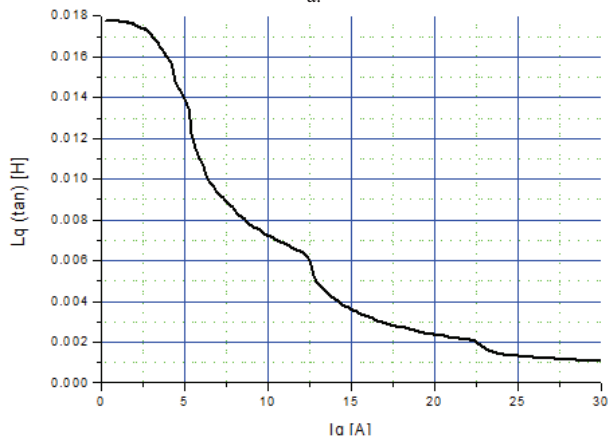
Fig. 18. a. Back-EMF, b. Cogging torque

From Fig. 18a, we can determine the peak value of the back-EMF ( $E_{pk}=22V$ ) and the peak value of the cogging torque ( $T_{cogg}=0,021Nm$ ). It can observe a decrease of the back-EMF of 8.33% comparing to the variant VPMSynRM-2V and the same value comparing to the variant VPMSynRM-2VU. For the peak values of the cogging torque, the variant with flux concentration rotor PMSM-FC has an increased value of 75% comparing to the variant VPMSynRM-2V and a diminution of 114% comparing to the variant VPMSynRM-2VU.

The curves of the simulated inductances  $L_d$  and  $L_q$  versus currents  $I_d$  and  $I_q$  are shown in the Fig. 19.



a.



b.

Fig. 19. a.  $L_d$  and b.  $L_q$  inductivities curves vs. currents

The curves of inductance were simulated using the FEM and the method described above using the relations (3), and (4).

For d- and q-axis inductance following values were obtained:  $L_d(4A) = 12.76$  mH,  $L_q(4A) = 15.91$  mH.

Fig. 20. presents the variation of torque caused by the permeance variations at 4.5A in the constant torque area. In this case for the proposed PMSM with concentration flux rotor at 5 A the average torque is  $T_{avPMSM-FC}=2.2$  Nm and the torque ripple is  $T_{ripplePMSM-FC}=26,3\%$ .

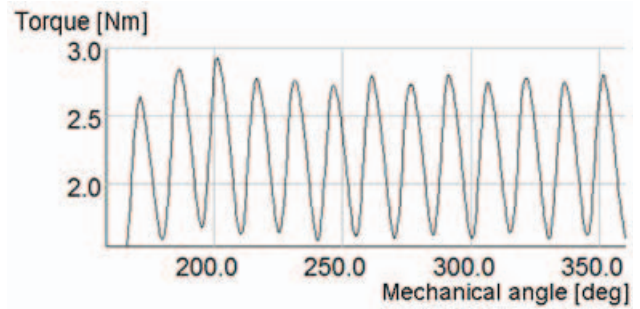


Fig. 20. Torque variation at 5.0 A.

In the TABLE I are listed the simulation results of the proposed solutions for the rotor geometry.

TABLE I.

	Rotor Type			
	PMSM-FC	1V	2V	2VU
$V_{PM}[mm^3]$	26481.72	39587.37	29325.04	24339.78
$L_d(4A)[mH]$	12.76	20.49	23.75	~23.75
$L_q(4A)[mH]$	15.91	11.96	15.8	~15.8
$L_d/L_q$	1.24	1.71	1.50	~1.50
$T_{av}/I[Nm/ Apk]$	2.2/5.0	1.2/3.45	1.9/3.45	~1.9/3.45
$T_{ripple}[\%]$	26.3	31	26.3	~26.3

## VII. EXPERIMENTAL RESULTS

The PMSM-FC rotor (see Fig. 21) has been manufactured and the experimental results were compared with the simulated results.



Fig. 21. PMSM with flux concentrator rotor PMSM-FC

In the TABLE II are listed the measured motor parameters of the PMSM-FC.



TABLE II.

$R_s[\Omega]$	$L_d[mH]$	$L_q[mH]$	$\Psi_{PM}[mWb]$
2,65	14,98	19,12	68,00

The measured values of the d- and q-axis inductance are different from the simulated values and the ratio  $L_q/L_d$  is better in the case of the measured values. This difference can be explained by the fact that the pole geometry was modified for a better fixation of the magnets. The difference between the simulated and the measured PM flux linkage is small, so we can say that simulated results have been validated by the experimental results.

The obtained prototype was also tested on the dyno. The electromechanical performances (motor current vs torque and efficiency vs torque) of the PMSM-FC are presented in Fig. 22 and Fig. 23.

### VIII CONCLUSIONS

This paper proposes two different low-cost ferrite solutions: first a V permanent magnet assisted synchronous reluctance rotor (VPMSynRM) and the second a permanent magnet synchronous with rotor flux concentrator PMSM-FC as an alternative solution to the rare earth inserted tangential permanent magnet synchronous motor (PMSM).

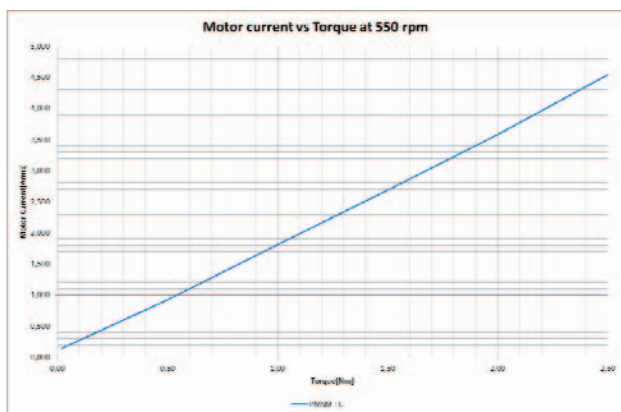


Fig. 22. Measured motor performance – Motor current vs torque.

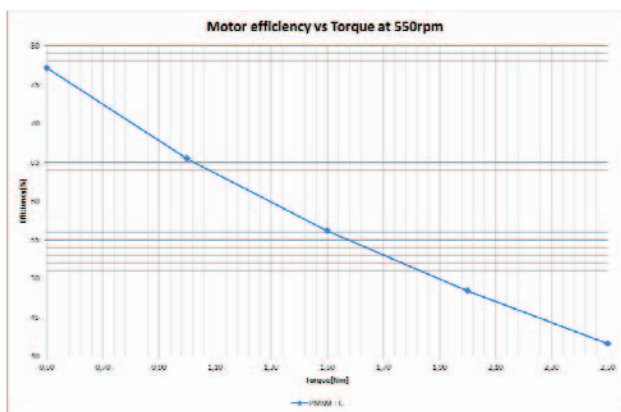


Fig. 23. Measured motor performance – Motor efficiency vs torque.

Finite element (FEM) approach has been utilized to show the performance of the proposed rotors. The PMSM-FC rotor was manufactured and the simulated results have been validated by the experimental results.

All these proposed rotor geometries with the flux barriers or flux concentrator and ferrites are attractive alternative solutions to reduce the cost of the rotor by changing the type of PM.

### REFERENCES

- [1] S. Musuroi, C. Sorandaru, M. Greconici, V.N. Olarescu, M. Weinman, „Low-cost ferrite permanent magnet assisted synchronous reluctance rotor an alternative for rare earth permanent synchronous motors”, Industrial Electronics Society, IECON 2013- 39th Annual Conference of the IEEE, 10-13 Nov. 2013, Vienna, pp. 2966-2970.
- [2] S. Morimoto, M. Sanada, Y. Takeda, and K. Taniguchi, “Optimum machine parameters and design of inverter driven synchronous motors for wide constant power operation,” in Conf. Rec. IEEE-IAS Annu. Meeting, 1994, pp. 177–182.
- [3] J. Cross, P. Viarouge, "Synthesis of High Performance PM Motors with Concentrated Windings," IEEE Transactions on Energy Conversion, vol. 17, no. 2, June 2002.
- [4] Vagati A., Fratta A., Franceschini G., Rosso P.M.: “A.C. motor for highperformance drives: a design-based comparison”, IEEE Trans. On Industry Applications, Sept.-Oct. 1996, vol. 32, n. 4, pp. 1211-1219.
- [5] H. Akita, Y. Nakahara, N. Miyake and T. Oikawa, "New Core Structure and Manufacturing Method for High Efficiency of Permanent Magnet Motors", Rec. of 2003 IEEE Industry Applications Society Annual Meeting, vol. 1, Salt Lake City, UT, October 2003, pp. 367-372.
- [6] Y. Takeda, N. Matsui, J. Oyama, and H. Domeki, “Classification and technical term of reluctance motors from the viewpoint of control strategy and motor construction,” in Proc. JIASC'02, vol. 2, 2002, pp. 759–762.
- [7] T.A. Lipo, A. Vagati, L. Malesani, and T. Fukao, “Synchronous reluctance motors and drives-a new alternative” IEEE-IAS Annual Meeting Tutorial, October 1992.
- [8] A. Vagati, M. Pastorelli, G. Franceschini, and S. C. Petrache, “Design of low-torque-ripple synchronous reluctance motors,” IEEE Trans. Ind. Appl., vol. 34, no. 4, pp. 758–765, Jul./Aug. 1998.
- [9] P. Niazi, H. A. Toliyat, D. H. Cheong, J. C. Kim, “A Low-Cost and Efficient Permanent-Magnet-Assisted Synchronous Reluctance Motor Drive” IEEE Transactions on Industry Applications, Vol.43, no2, (2007).
- [10] S. Talebi, P. Niazi, H.A.Toliyat, “Design of Permanent Magnet-Assisted Synchronous Reluctance Motors Made” Easy”, 42nd IAS Annual Meeting. Conference Record of the 2007 IEEE, 23-27 Sept. 2007, pp. 2242 – 2248.
- [11] T. Matsuo and T. A. Lipo, “Rotor design optimization of synchronous reluctance machine,” IEEE Trans. Energy Conversion, vol. 9, pp. 359–356, June 1994.
- [12] S.A. Long, N. Schofield, D. Howe, M. Piron, M. McClelland, “Design of a switched reluctance machine for extended speed operation”, IEEE Proc.of IEMDC03, pp235-240.
- [13] E. Armando, P. Guglielmi, M. Pastorelli, G. Pellegrino, and A. Vagati, “Accurate Magnetic Modelling and Performance Analysis of IPMPMASR Motors”, IEEE-IAS Annual Meeting, 23-27 Sept. 2007, New Orleans (USA), pp. 133 – 140.
- [14] N. Bianchi, Electrical Machine Analysis Using Finite Elements, ser. Power Electronics and Applications Series. Boca Raton, FL: CRC Press, 2005
- [15] E.E. Montalvo-Ortiz, S.N. Foster, J.G. Cintron-Rivera, E.G. Strangas, “Comparison between a spoke-type PMSM and a PMASynRM using ferrite magnets”, Electric Machines & Drives Conference IEMDC 2013, 12-15 May, 2013, Chicago IL, pp.1080-1087.
- [16] P. Guglielmi, B. Boazzo, E. Armando, G. Pellegrino and A. Vagati, “Permanent-Magnet Minimization in PM-Assisted Synchronous Reluctance Motors for Wide Speed Range”, IEEE Transactions on Industry Applications, vol. 49, no. 1, pp. 31-41, January/February 2013.
- [17] R. Magureanu, “Special Electric Machines for automated systems”, Tenica Publishing House, Bucharest, 1981.